Electronic Supplementary Material (ESI) for Journal of Materials Chemistry C.

# Solution-Processed Copper Arsenic Sulfide Thin Films for Photovoltaic Applications

*Scott A. McClary*, Joseph Andler**, Carol A. Handwerker**, Rakesh Agrawal**

*Davidson School of Chemical Engineering, Purdue University, 480 Stadium Mall Drive, West Lafayette, IN 47907.

**School of Materials Engineering, Purdue University, 701 West Stadium Avenue, West Lafayette, IN 47907.

# Supporting Information

## Experimental Methods

***Caution: Arsenic compounds are highly toxic and must be handled with extreme caution and appropriate personal protective equipment after consulting the safety data sheets for each material. In particular, arsenic trichloride ($AsCl_3$) MUST be handled under an inert environment at all times. Specific data on the toxicity of $Cu_3AsS_4$ is not available, so it should also be handled with the utmost care.***

*Materials:* All raw materials were used as received with standard air-free techniques unless otherwise noted. Sulfur flakes (S, 99.99%), arsenic (III) chloride ($AsCl_3$, 99.99%), arsenic (As, 99.997%), arsenic (III) sulfide ($As_2S_3$, 99.99%), oleylamine (OLA, >98% primary amine), 1-hexanethiol (HT, 95%), and ammonium sulfide ($(NH_4)_2S$, 40-48 wt% in water) were obtained from Sigma-Aldrich. OLA was degassed using three freeze-pump-thaw (FPT) cycles and stored under nitrogen prior to use in synthesis. Arsenic (V) sulfide ($As_2S_5$, >98%) was obtained from Santa Cruz Biotechnology. Copper (I) chloride (CuCl, 99.99%) was obtained from Strem. Ammonium hydroxide ($NH_4OH$, 28-30 wt% in water) was obtained from J.T. Baker. Hexanes (98.5%) were obtained from Fisher. Ethanol (200 proof) was obtained from Koptec. Acetone (99.5%) was obtained from EM Science.

*Nanoparticle Synthesis:* Nanoparticles (NPs) were synthesized according to the recipe of Balow et al. scaled up 50% with a modified washing procedure.[1] Briefly, solutions of 1 M S in FPT OLA and 0.2 M CuCl/$AsCl_3$ in FPT OLA (2.8:1 Cu:As ratio, concentration refers to Cu only) were prepared by heating to 65 °C and stirring for 2 h under nitrogen before use. A three-neck flask consisting of 10.5 mL non-FPT OLA was refluxed at 120 °C for 1 h to remove dissolved gases and then heated to 175 °C. Then, 1.2 mL of S-OLA solution was injected, followed by 3.0 mL of CuCl/$AsCl_3$-OLA solution 20 s later. The reaction proceeded for 10 min and was then cooled via natural convection to room temperature. The mixture was then extracted into a centrifuge tube, topped with ethanol, and centrifuged at 14 krpm for 5 min. The supernatant was discarded, and two more washes were performed with a ~1:3 v:v mixture of hexane and ethanol. After washing, particles were dried under nitrogen flow and stored for later use. The as-synthesized NPs are slightly copper poor (2.6-3.0 Cu:As ratio) and sulfur rich (3.9-4.5 S:As ratio) and are expected to average between 7-8 nm in diameter in agreement with previous reports.[1,2]

*Film Fabrication:* NP films were cast by dispersing NPs in HT at 250 mg/mL and then doctor blading the resulting NP "ink" onto a 2" by 1" molybdenum-coated soda-lime glass (Mo-SLG) substrate. One coat of 15 µL ink was applied and dried at room temperature for five minutes. Then, another coat of 10 µL was applied followed by overnight drying before use.

*Ampoule Preparation:* NP samples (cut to ¼" by 1") and powders (by experiment: $As_2S_5$ – 37 mg, S – 10.8 mg, As – 9.9 mg, S and As – 19.7 and 18.4 mg, respectively) were placed in a ChemGlass 10 mL borosilicate glass type 1 ampoule, which was then attached to a Schlenk line. The ampoule was evacuated and refilled with argon three times. It was then evacuated again to a pressure below 100 mtorr, and the neck was slowly rotated through a butane flame to collapse the glass walls and form a seal. *For safety reasons, the amounts of added powders were chosen such that the total pressure inside the ampoule would not exceed 0.8 atm, assuming that all solid vaporized into an ideal gas.*

*Annealing Treatments and Device Fabrication:* Sealed ampoules were heated individually in a horizontal tube furnace under 10 sccm argon flow. Each ampoule was pushed into the furnace after the temperature had reached the desired setpoint; once the treatment was completed, the furnace was opened and cooled by natural convection. Afterwards, ampoules were broken in the ambient atmosphere by scribing around the neck with a diamond-tip pen and snapping them forcefully. At this point, samples were either characterized or processed into full devices. Additional solar cell device layers were applied using chemical bath deposition of ~50 nm CdS, RF-sputtering of ~80 nm i-ZnO, RF-sputtering of ~220 nm ITO, and electron beam evaporation of patterned Ni/Al grids. The grids resulted in separate cells that had an area of 0.1 $cm^2$; these cells were electrically isolated from each other by mechanical scribing.

*Ligand Exchange:* In order to further investigate the effects of ligands on the formation of the 494 $cm^{-1}$ and other peaks in the Raman spectrum of treated NPs (as discussed in the body of the manuscript), carbonaceous OLA ligands were replaced with an $As_2S_3$-based molecular metal chalcogenide complex using a ligand exchange procedure adapted from the method of Kovalenko et al.[3] To synthesize $(NH_4)_3AsS_3$, 246 mg (1 mmol) $As_2S_3$ was vigorously stirred with 0.43 mL $(NH_4)_2S$ and 5 mL ultrapure water until complete dissolution occurred (~24 h). The mixture was then mechanically filtered using a 10 µm PTFE filter. To conduct the ligand exchange, a newly-synthesized batch of luzonite (LUZ) $Cu_3AsS_4$ NPs was diluted to 25 mg/mL in toluene. 1 mL of this toluene suspension was vortexed with 6 mL hexane in a centrifuge tube, along with a Teflon-coated stir bar. The mixture was taken into a nitrogen-filled glovebox, where 6 mL of $NH_4OH$ and 1 mL of the $(NH_4)_3AsS_3$ solution were added. The mixture was vigorously stirred on a magnetic stir plate for 90 min, at which point the NPs had transferred from the nonpolar organic phase to the polar aqueous phase, indicating that a successful ligand exchange had occurred. The clear nonpolar supernatant was drawn off, 7 mL hexane was added, and the mixture was stirred again for 1 h to remove any residual OLA from the nanoparticles. The hexane mixture was drawn off again, and the particles were centrifuged at 14 krpm for 5 min in the presence of 10 mL water and 10 mL acetone mixtures.

*Treatments with Ligand Exchanged Particles:* The ligand-exchanged nanoparticles were diluted to 10 mg/mL with water and spray coated onto a 1” by 1” Mo-SLG substrate held at a temperature of 150 °C. The substrate was then cut to ¼” by 1” and sealed in an ampoule with added $As_2S_5$, as described in the “Ampoule Preparation” section. The ampoule was heated at 425 °C for 1 h and cooled in accordance with other treatments. The substrate was then characterized. 50 µL OLA was then drop-cast on the surface and allowed to dry overnight. This sample was sealed in an ampoule with sulfur and treated again for 1 h at 425 °C.

*Characterization:* XRD data were collected on a Rigaku SmartLab diffractometer using a copper Kα X-ray source in Bragg-Brentano mode. Raman spectra were taken using a Horiba/Jobin-Yvon LabRAM HR800 confocal microscope system with a 17 mW 633 nm He:Ne laser. SEM and EDX were conducted on an FEI Quanta electron microscope equipped with a silicon drift EDX detector, and elemental compositions were obtained with AzTEC software using a standardless quantitative analysis based on the Cliff-Lorimer method. SEM images and EDX measurements were taken at accelerating voltages of 7 kV and 20 kV, respectively. TGA was conducted using a TA Instruments SDT Q600 system in a 100 mL/min helium flow at a ramp rate of 10°C/min. The J-V measurements were acquired with an Oriel Sol3A solar simulator with the AM1.5G spectrum calibrated to 100 mW/cm$^2$ using a certified silicon reference cell. External quantum efficiency (EQE) measurements were performed at 160 Hz and zero bias using a lock-in amplifier and preamplifier for signal processing.

## Supplemental Figures and Tables

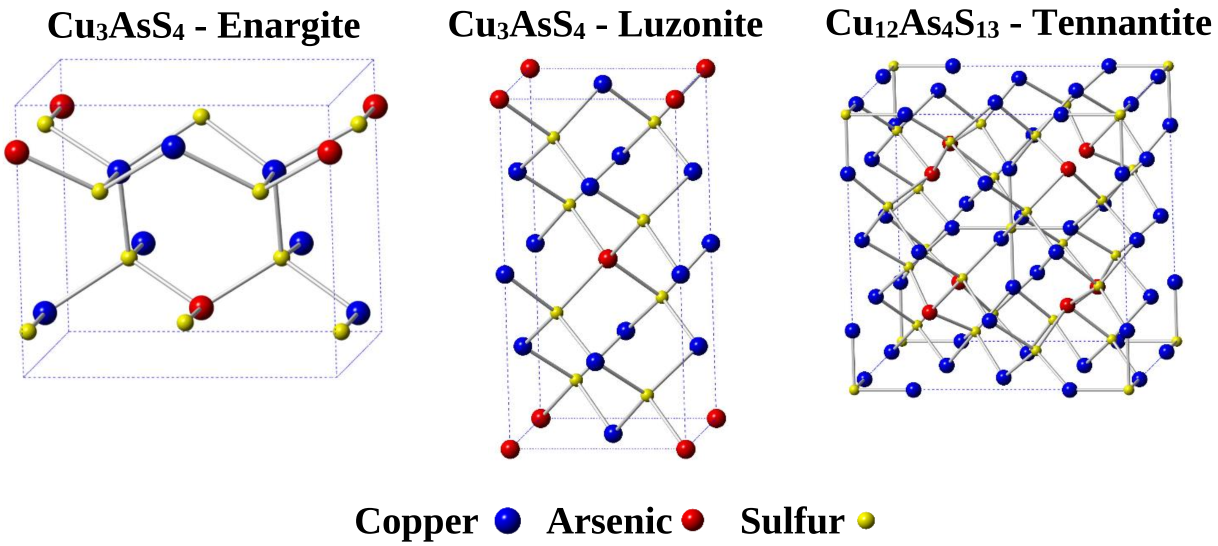

$Cu_3AsS_4$ - Enargite

$Cu_3AsS_4$ - Luzonite

$Cu_{12}As_4S_{13}$ - Tennantite

**Figure S1.** Crystal structures and compositions of three copper-arsenic-sulfur structures encountered in this work.

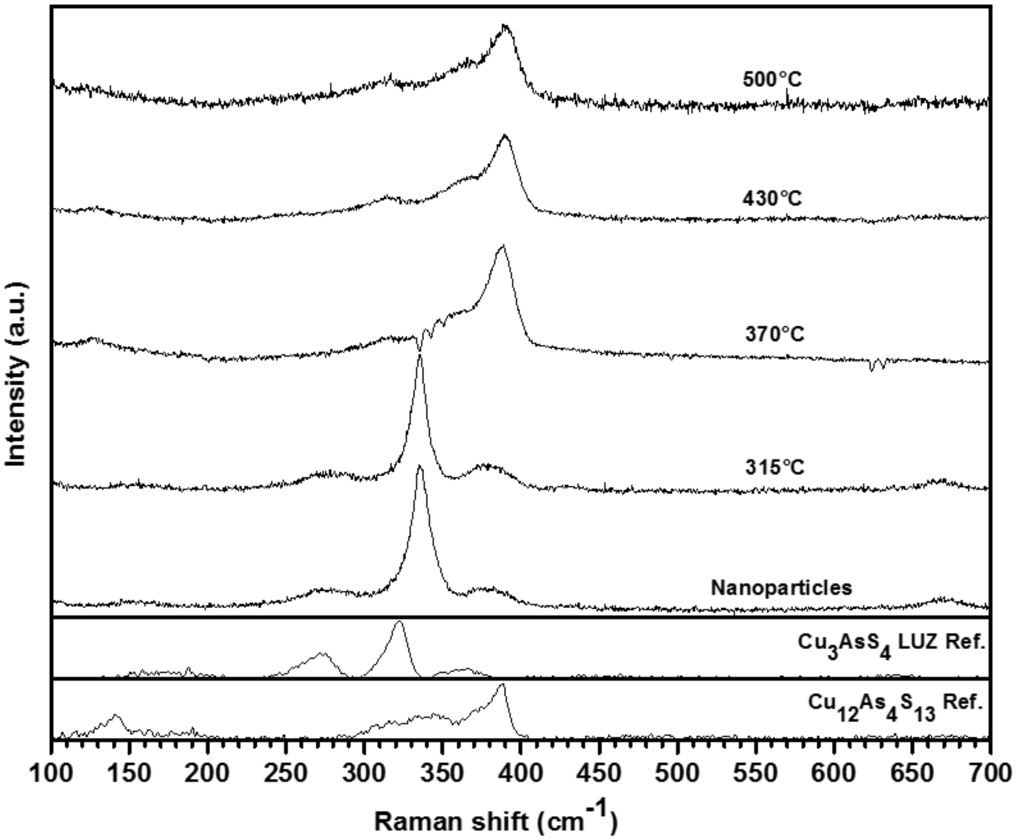

**Figure S2.** Raman spectra of luzonite NP films heated to the indicated temperature. A clear phase transition from luzonite to tennantite is noted between 315 °C and 370 °C. The nanoparticle and 315 °C spectra are noticeably shifted from the $Cu_3AsS_4$ LUZ reference (RRUFF ID R060390) due to antimony in the reference spectrum. ($Cu_{12}As_4S_{13}$ reference: RRUFF ID R050474)

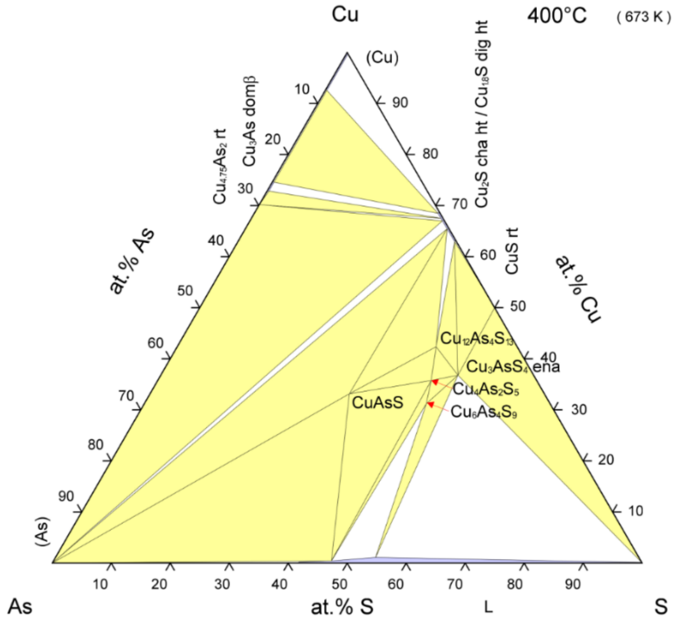

© ASM International 2006. Diagram No. 976807

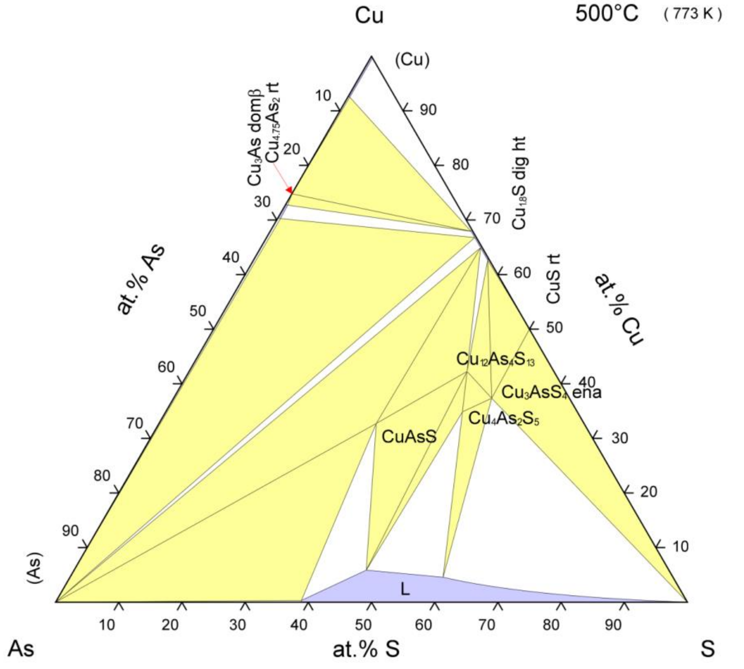

© ASM International 2006. Diagram No. 976805

**Figure S3.** Ternary isothermal sections of the Cu-As-S system at 400 °C and 500 °C, adapted from Maske and Skinner.[4] Diagrams copyright ASM International (2006) and reprinted with permission.[5]

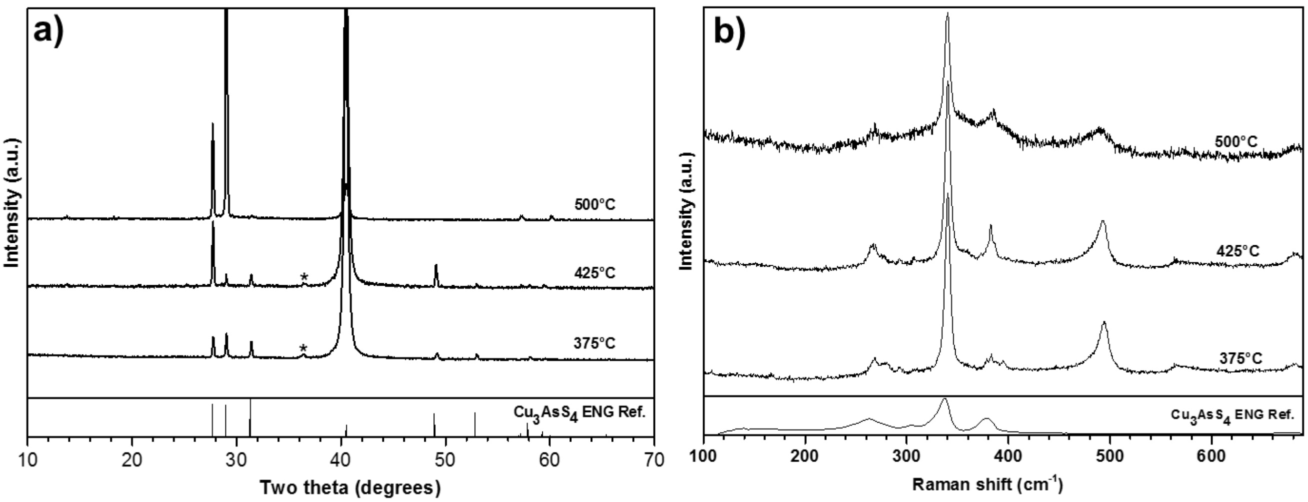

**Figure S4.** a) XRD and b) Raman spectra of luzonite NP films treated at 375, 425, and 500 °C for 1 h. In the XRD spectra, the peak locations match well with those of an ENG reference mineral (JCPDS 01-082-1464) with overly dominant intensities attributed to oriented growth. The peak at 40° is indexed to the Mo substrate and the peak at 36.5° (*) is attributed to incomplete filtering of the k-beta radiation from the Mo peak. In the Raman spectra, the stretches also match well with an enargite reference (RRUFF ID: R050373) with an additional peak at 494 cm$^{-1}$, the origins of which are discussed in the body of the article.

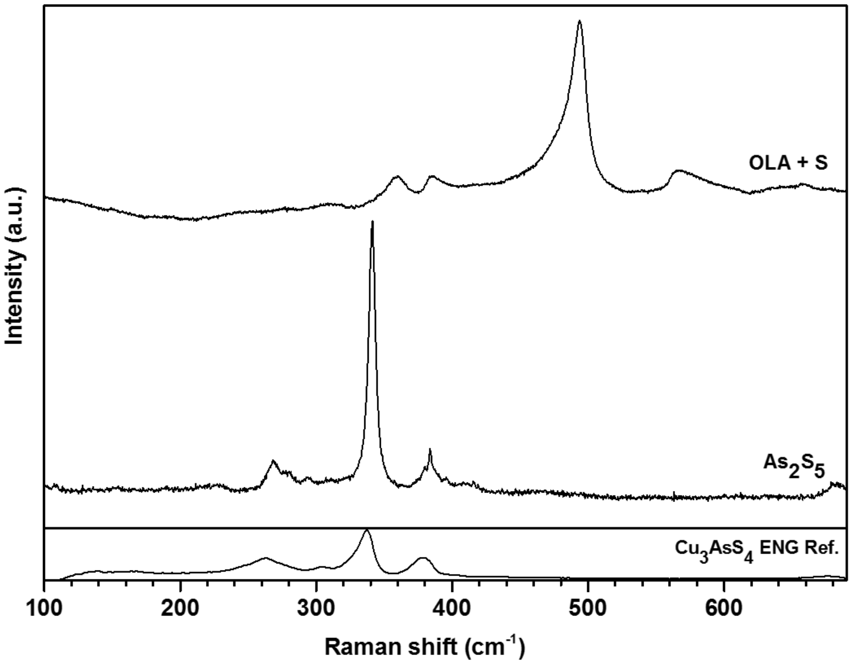

**Figure S5.** Raman spectra of ligand-exchanged luzonite $Cu_3AsS_4$ NPs. The NPs were treated first in $As_2S_5$ at 425 °C for 1 h, showing no trace of the peak at 494 cm$^{-1}$ seen in materials with OLA-capped particles. Then, OLA was drop-cast on the surface of the treated film, which was was treated in sulfur at 425 °C for 60 minutes, resulting in the Raman spectrum with peaks at 360, 494, and 560 cm$^{-1}$ that may be attributed to the impurity phase; the peak around 380 cm$^{-1}$ may be attributed to tennantite $Cu_{12}As_4S_{13}$ or also to the impurity phase. EDX measurements taken on the top of the sample at an accelerating voltage of 20 kV showed only carbon and sulfur in the OLA/S-treated films.

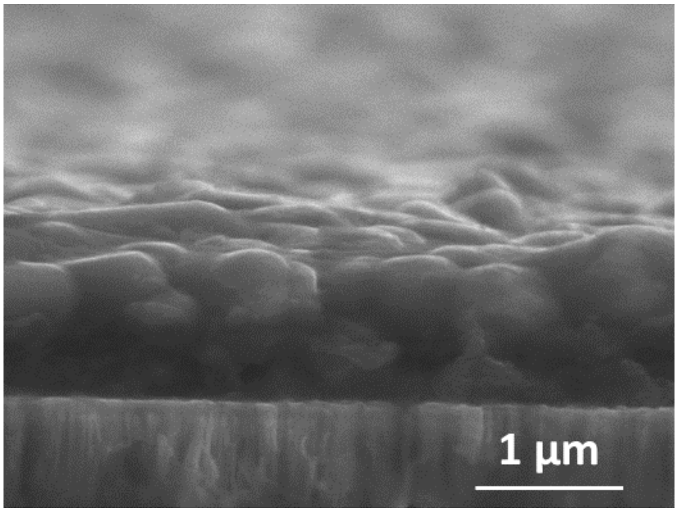

**Figure S6.** Side-view SEM image of LUZ NP film treated in a sealed ampoule with $As_2S_5$ powder for 1 h at 425 °C. A thin fine-grain layer and some contrast in the molybdenum are noted.

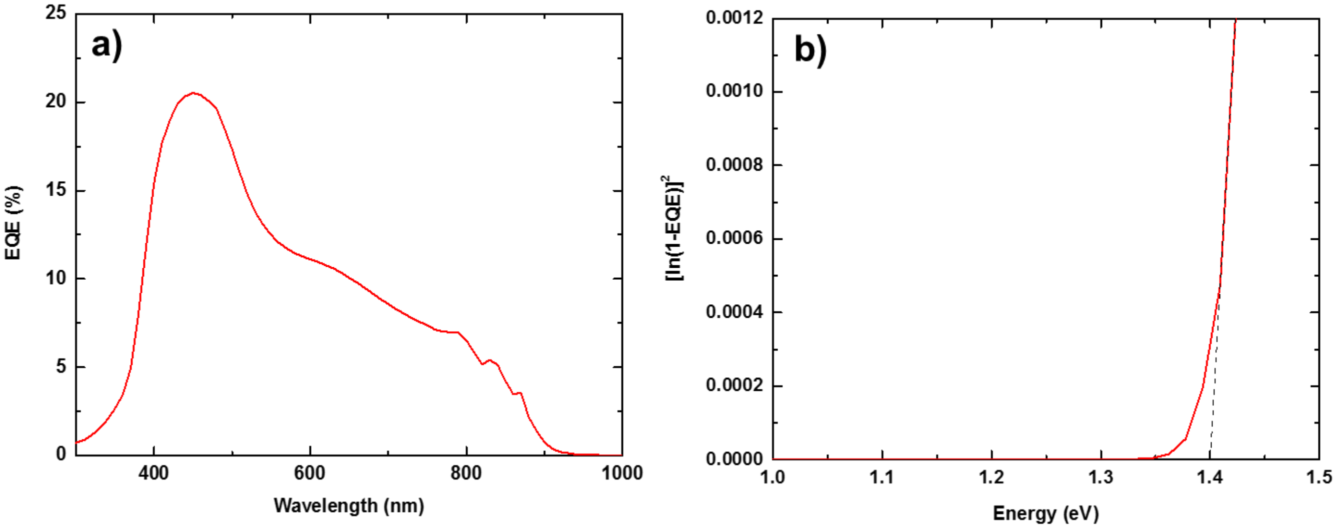

Figure S7. a) External quantum efficiency (EQE) measurements of the device shown in Figure 4 in the main text of the manuscript. When integrated, a $J_{sc}$ of 3.4 mA/cm$^2$ is obtained, which agrees well with the value (3.3 mA/cm$^2$) obtained from J-V measurements. 2.2 mA/cm$^2$ of this current occurs at wavelengths greater than 510 nm (or below 2.43 eV, the approximate band gap of CdS) and is therefore attributed to carrier generation in the $Cu_3AsS_4$ absorber layer only. b) Extrapolation of band gap energy through a plot of $[\ln(1\text{-EQE})]^2$ vs photon energy. A band gap of 1.4 eV is obtained in agreement with a previous experimental result.[6]

**Table S1.** EDX compositions measured for NP samples treated at 375 °C, 425 °C, and 500 °C with $As_2S_5$ for 1 h. The measured ratios indicate that arsenic and sulfur have incorporated into the film beyond the target 3:1 Cu:As and 0.75 Cu:S ratios.

| | **375 °C** | **425 °C** | **500 °C** |
|---|---|---|---|
| **Cu:As** | 1.83 | 2.04 | 2.29 |
| **S:As** | 4.41 | 3.94 | 4.15 |
| **Cu:S** | 0.42 | 0.52 | 0.55 |

**Table S2.** Device statistics (n = 10) for solar cells based on a common ENG absorber layer (cell area = 0.1 cm$^2$). Out of the ten devices, one had a fill factor and efficiency of 0%. The second set of columns represents the device statistics without this particular device included (n = 9).

| | **n = 10** | | **n = 9** | |
|---|---|---|---|---|
| | **Average** | **St. Dev.** | **Average** | **St. Dev.** |
| **$V_{oc}$ (V)** | 0.12 | 0.07 | 0.13 | 0.07 |
| **$J_{sc}$ (mA cm$^{-2}$)** | 2.3 | 1.2 | 2.5 | 1.1 |
| **FF (%)** | 24.0 | 8.3 | 26.7 | 2.4 |
| **Efficiency (%)** | 0.08 | 0.06 | 0.09 | 0.06 |

## Investigation of Varying Annealing Atmosphere on Grain Structure

Elemental sulfur and arsenic were compared with $As_2S_5$ as vapor sources for LUZ NP films at 425 °C for 1 h. Under such conditions, different growth mechanisms are expected because there is no pathway to a Cu-containing ternary liquid phase (Figure S3). A sulfur atmosphere facilitated heterogeneous grain formation (Figure S8a) of the tetragonal LUZ crystal structure (Figure S9). This is a surprising result, as LUZ was previously reported to convert to ENG by 320 °C.[4] In contrast, arsenic alone resulted in a few isolated grains and a highly cracked film (Figure S8b). Under these conditions, the film converted to the sulfur-deficient TEN structure (Figure S9) as expected.

In a separate experiment, both elemental As and S were added in a 2:5 molar ratio for comparison with the $As_2S_5$ additive. When LUZ NPs were treated at 425 °C for 1 h, the grain size distribution was quite different – isolated, large grains formed on the surface with a dense network of smaller grains filling the remaining space (Figure S8c). This phenomenon may be explained by different annealing environments seen with different ampoule additives. For instance, elemental sulfur will fill the vapor space more quickly than a binary compound will due to its higher vapor pressure, thereby introducing a more sulfur-rich environment at the early stages of grain development. Further investigation is needed to determine the precise environments seen by the NPs and to understand their effects on grain growth. When the $As_2S_5$

and elemental atmosphere experiments are considered jointly, it is evident that a binary As-S compound must be externally supplied to facilitate the growth of unimodal micron-sized dense grains.

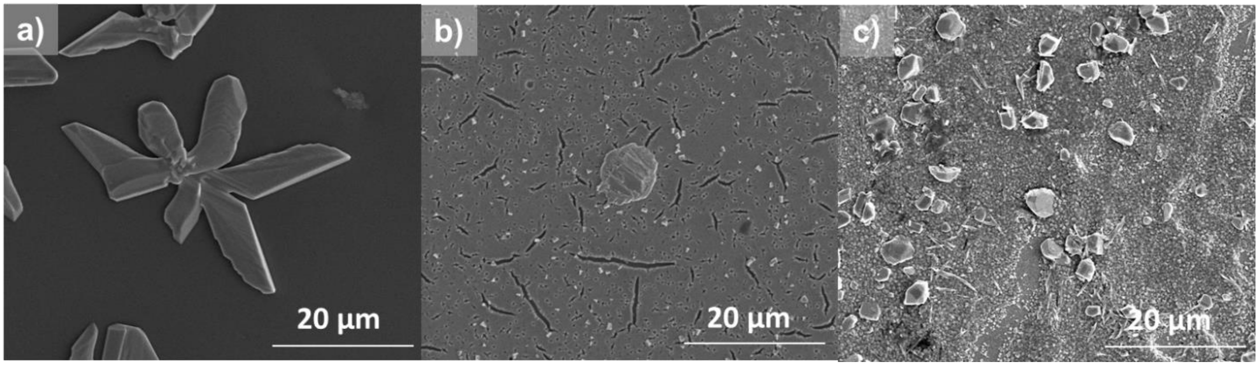

**Figure S8.** SEM images of LUZ NPs treated at 425 °C for 1 h in varying atmospheres: a) S, b) As, and c) As and S in a 2:5 molar ratio.

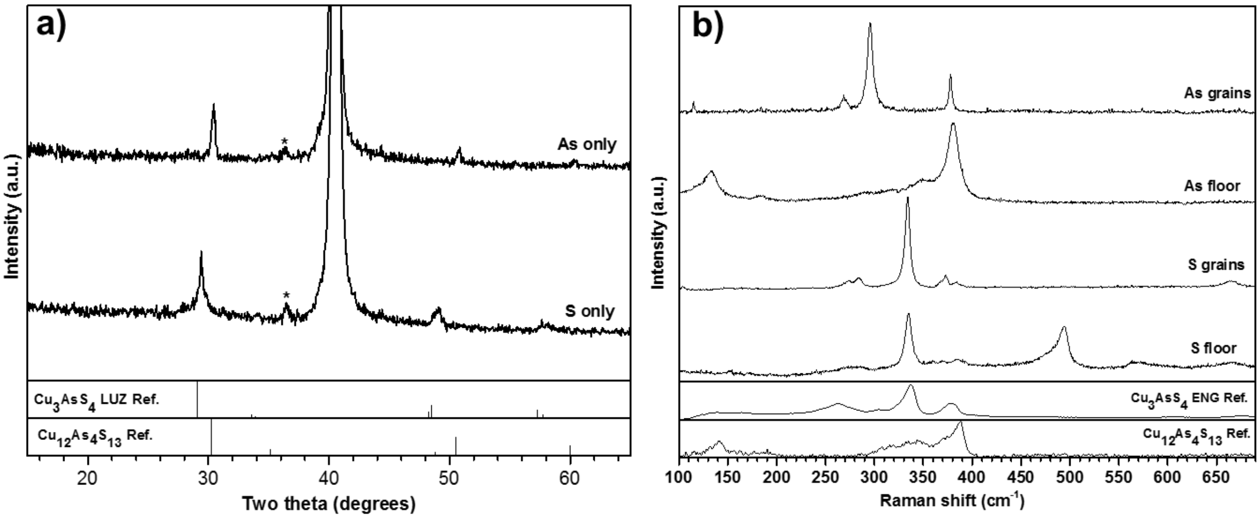

**Figure S9.** a) XRD and b) Raman spectra of LUZ NPs treated in separate sulfur and arsenic atmospheres. In the XRD spectrum, the sulfur-treated film matches well with a tetragonal luzonite reference (JCPDS 01-074-1125), with shifts due to antimony in the reference spectrum. The arsenic-treated film, however, matches with the cubic tennantite $Cu_{12}As_4S_{13}$ reference (JCPDS 42-560). In both, the peaks at 40° are indexed to the Mo substrate and the peaks at 36.5° (*) are attributed to incomplete filtering of the k-beta radiation from the Mo peaks. In the Raman spectra, the large size of the grains made it possible to take data on both the grains and the background “floor” layer. Both sulfur-treated spectra match well with enargite $Cu_3AsS_4$ (RRUFF ID: R050373) or luzonite $Cu_3AsS_4$ (RRUFF ID R060390, not shown) references, though there are additional impurity peaks only seen in the floor grains. The arsenic-treated “floor” layer matches with a reference tennantite $Cu_{12}As_4S_{13}$ mineral (RRUFF ID: R050474); the grains, however, do not match with a recorded spectrum of binary or ternary Cu-As-S phases. Due to EDX measurements, we suspect that the grains are the lautite CuAsS phase, which, to the best of our knowledge, does not have a reported Raman spectrum.

References

1 R. B. Balow, E. J. Sheets, M. M. Abu-Omar and R. Agrawal, Chem. Mater., 2015, 27, 2290–2293.

2 R. B. Balow, C. K. Miskin, M. M. Abu-Omar and R. Agrawal, Chem. Mater., 2017, 29, 573–578.

3 M. V. Kovalenko, M. I. Bodnarchuk, J. Zaumseil, J.-S. Lee and D. V. Talapin, J. Am. Chem. Soc., 2010, 132, 10085–10092.

4 S. Maske and B. J. Skinner, Econ. Geol., 1971, 66, 901–918.

5 Maske, S. and Skinner, B.J. As-Cu-S Phase Diagram, ASM Alloy Phase Diagram Database, P. Villars, editor-in-chief; H. Okamoto and K. Cenzual, section editors; http://mio.asminternational.org/apd/, ASM International, Materials Park, OH, 2006.

6 T.Pauporté and D. Lincot, Adv. Mater. Opt. Electron., 1995, 5, 289–298.